Наносистеми, наноматеріали, нанотехнології
Nanosistemi, Nanomateriali, Nanotehnologii
2025, т. 23, № 2, сс. 437–448
https://doi.org/10.15407/nnn.23.02.0437

PACS numbers: 61.72.Mm, 68.37.Ps, 68.55.J-, 78.55.Hx, 78.60.Lc, 81.15.Cd, 81.40.Tv

Surface Morphology and Low-Temperature Luminescence of Thin $(Y_{0.06}Ga_{0.94})_2O_3:Cr^{3+}$ Films

O. M. Bordun[1], I. O. Bordun[1], I. I. Medvid[1], D. M. Maksymchuk[1], I. Yo. Kucharskyy[1], I. M. Kofliuk[1], and D. S Leonov[2]

[1]*Ivan Franko National University of Lviv,*
50, Drahomanov Str.,
UA-79005 Lviv, Ukraine
[2]*Technical Centre, N.A.S. of Ukraine,*
13, Pokrovska Str.,
UA-04070 Kyiv, Ukraine

Thin films of $(Y_{0.06}Ga_{0.94})_2O_3$:Cr are obtained by radio-frequency (RF) ion-plasma sputtering in an argon atmosphere on amorphous υ-SiO_2 substrates. The surface morphology of the obtained films is studied by means of AFM. The low-temperature (8.6 K) luminescence of the thin films of $(Y_{0.06}Ga_{0.94})_2O_3:Cr^{3+}$ under excitation by synchrotron radiation (22.14 eV and 7.75 eV) is studied. The obtained luminescence spectra are analysed according to excitation energy. A high-energy shift of the R_1-line in the spectra of the activator luminescence of the Cr^{3+} ion in the thin films of $(Y_{0.06}Ga_{0.94})_2O_3:Cr^{3+}$ is found relative to the same for single crystal samples. This shift is analysed in the form of a nephelauxetic effect.

Методом високочастотного (ВЧ) йонно-плазмового розпорошення в атмосфері арґону на аморфних підкладинках υ-SiO_2 одержано тонкі плівки $(Y_{0,06}Ga_{0,94})_2O_3$:Cr. Методом АСМ досліджено морфологію поверхні одержаних плівок. Проведено дослідження низькотемпературної (8,6 К) люмінесценції тонких плівок $(Y_{0,06}Ga_{0,94})_2O_3:Cr^{3+}$ через збудження синхротронним випромінюванням (22,14 еВ і 7,75 еВ). Проаналізовано одержані спектри люмінесценції залежно від енергії збудження. Встановлено високоенергетичне зміщення R_1-лінії у спектрах активаторного свічення йона Cr^{3+} у тонких плівках $(Y_{0,06}Ga_{0,94})_2O_3$:Cr відносно такої для монокристалічних зразків. Дане зміщення проаналізовано у формі нефелоксетичного ефекту.

Key words: gallium oxide, yttrium oxide, chromium activator, thin films, nanocrystals, photoluminescence, synchrotron radiation.

Ключові слова: оксид Ґалію, оксид Ітрію, активаторний Хром, тонкі плі-

вки, нанокристаліти, фотолюмінесценція, синхротронне випромінення.

(Received 16 April, 2025)

1. INTRODUCTION

In recent years, oxide nanostructures based on β-Ga_2O_3 have been extensively studied. This material, which belongs to wide bandgap semiconductors, is widely used in ultraviolet photodetectors, gas sensors, solar cells, luminescent devices, and high-power Schottky diodes [1–8]. Due to their operational and chemical properties, pure and activated nanometre thin films of β-Ga_2O_3 obtained by various methods are widely used in luminescent devices. Among them, an important place is occupied by β-Ga_2O_3:Cr^{3+} as a red phosphor for multiple types of luminescent screens, including flat panel PDP (plasma, display, panel) screens [9–13].

In general, the optical and luminescent properties of thin oxide films, including β-Ga_2O_3:Cr^{3+}, are determined by the methods of preparation, deposition modes, processing technology, and the introduction of special impurities that can purposefully change the spectral and luminescent properties of the films. Given that the luminescence of β-Ga_2O_3 depends significantly on structural defects [14–16], in this work, some Ga^{3+} ions were replaced by isovalent Y^{3+} ions, which did not require local compensation of the electric charge. At the same time, it was taken into account that Y_2O_3 thin films are quite promising when used in optoelectronics and luminescent technology [17–20]. This led to the study of thin films with the chemical composition $(Y_{0.06}Ga_{0.94})_2O_3$:Cr^{3+} in this work.

Taking into account that the physical properties of thin films are determined by the size of the nanocrystalline grains from which they are formed and the presence of intergranular boundaries, the surface morphology of thin $(Y_{0.06}Ga_{0.94})_2O_3$:Cr^{3+} films was studied by atomic force microscopy (AFM). In order to study in detail the luminescence in these films, the luminescence spectra were studied under excitation by synchrotron radiation at low temperatures $T = 8.6$ K. The films were obtained by the method of RF ion-plasma sputtering, which is considered optimal for depositing homogeneous multicomponent semiconductor and dielectric films [21].

2. EXPERIMENTAL TECHNIQUE

Thin films of $(Y_{0.06}Ga_{0.94})_2O_3$:Cr with a thickness of 0.3–1.0 μm were obtained by RF ion-plasma sputtering in an argon atmosphere on amorphous substrates of fused quartz υ-SiO_2. The feedstock was a

mixture of Y_2O_3 and Ga_2O_3 oxides of the stoichiometric composition of the 'ОСЧ' (especially pure) grade. The concentration of the activator ion Cr^{3+} was 0.5 mol.%. After the films were deposited, they were heat treated in argon at 1000–1100°C.

The structure and phase composition of the obtained films were studied by x-ray diffraction analysis (Shimadzu XDR-600). X-ray diffraction studies have shown the presence of a polycrystalline structure with a predominant orientation in the (002), (111), (110), and (512) planes. The analysis of the obtained diffractograms shows that the structure of the films corresponds to the monoclinic crystal structure of β-Ga_2O_3.

At the same time, the obtained diffractograms practically coincide with the diffractograms of unalloyed films of $(Y_{0.06}Ga_{0.94})_2O_3$, which were presented earlier in our work [22].

Using an OXFORD INCA Energy 350 energy dispersive spectrometer, elemental analysis of the samples was carried out at several points on the surface of the films. The calculations showed that the percentage of components in the obtained films corresponded to their percentage in the $(Y_{0.06}Ga_{0.94})_2O_3$:Cr compound.

The surface morphology of the thin films was studied using an INTEGRA TS-150 atomic force microscope (AFM). The image of the thin film surface was obtained in the semi-contact mode.

The luminescence spectra at $T = 8.6$ K were studied using synchrotron radiation at the Superlumi facility (DESY, Hamburg, Germany) [23]. A primary monochromator with a spectral resolution of 4 Å was used to select the spectral range of synchrotron radiation for luminescence excitation. The luminescence spectra were recorded and analysed using an ANDOR Kymera monochromator with a spectral resolution of 2 Å, a Newton 920 CCD camera, and a Hamamatsu R6358 photoelectronic multiplier.

3. RESULTS AND DISCUSSION

Microphotographs of the surface of thin $(Y_{0.06}Ga_{0.94})_2O_3$:Cr films are shown in Fig. 1.

The topography of the samples was quantitatively characterized by standard parameters: root mean square roughness, maximum grain height, and average grain diameter, which were calculated from AFM data using Image Analysis 3.5 image processing software for a 5000×5000 nm area.

Based on the analysis of the surface morphology images, it was found that thin films of $(Y_{0.06}Ga_{0.94})_2O_3$:Cr after argon heat treatment have an average square surface roughness of 2.9 nm with a maximum grain height of 33 nm. The average grain diameter is of 123 nm.

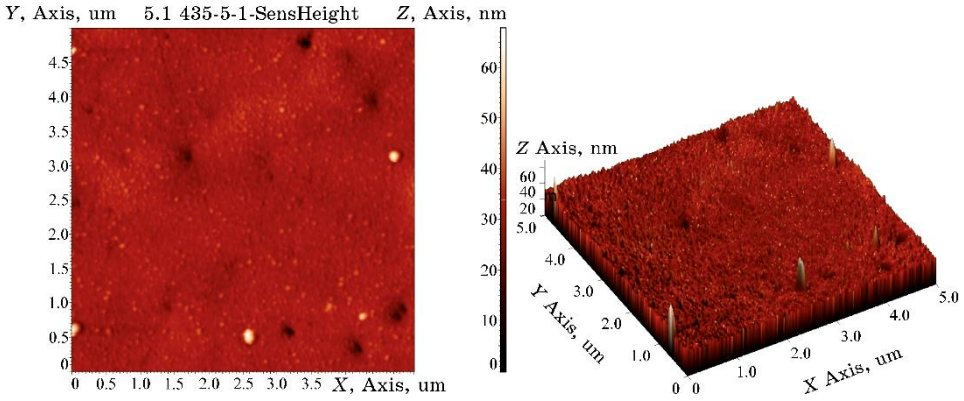

Fig. 1. Images of the surface morphology of thin $(Y_{0.06}Ga_{0.94})_2O_3$:Cr films after heat treatment in an argon atmosphere on υ-SiO_2 substrates. *a*—two-dimensional image; *b*—three-dimensional image.

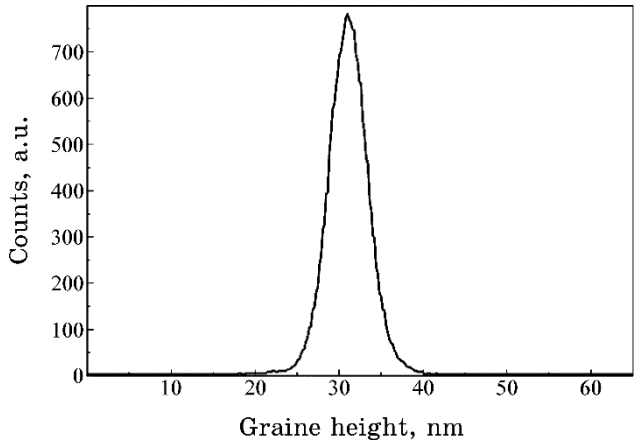

Fig. 2. Grain height distribution for AFM images of the surface of thin $(Y_{0.06}Ga_{0.94})_2O_3$:Cr films after heat treatment in an argon atmosphere.

The histogram of grain height distribution for the obtained films is shown in Fig. 2.

The characteristic distribution of grain diameter sizes in thin $(Y_{0.06}Ga_{0.94})_2O_3$:Cr films is shown in Fig. 3.

As can be seen in Fig. 3, the distribution of grain diameters in the obtained thin films has the form of a bimodal distribution. The growth of crystalline grains and the evolution of crystal structures were analysed in a thorough review [24], and it was shown that polycrystalline thin films with a thickness of up to 1 μm, which is typical for our $(Y_{0.06}Ga_{0.94})_2O_3$:Cr films, often have 2*D*-like struc-

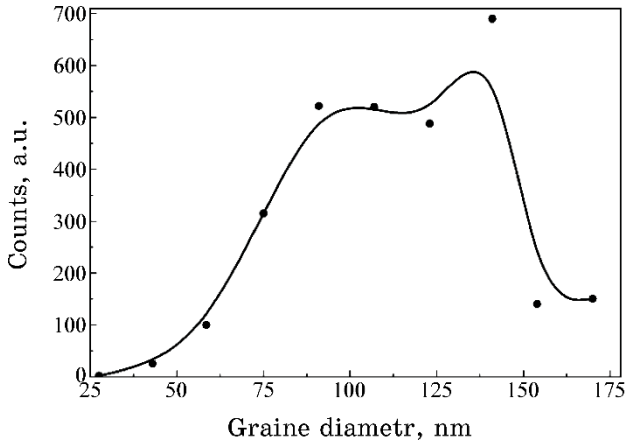

Fig. 3. Distribution of grain diameter sizes and calculated approximate diameter distribution on AFM images of thin $(Y_{0.06}Ga_{0.94})_2O_3$:Cr films after heat treatment in argon atmosphere.

tures. Most of the materials analysed in Ref. [24] form thin films of nonequilibrium grains, whose dimensions are smaller than the film thickness, and they form two-dimensional structures only after annealing. In some cases, further grain growth is observed due to 'anomalous' growth or preferential coalescence of several grains, which usually have specific crystallographic orientations and ratios relative to the substrate surface plane. Our results show that such a situation is most likely characteristic of the $(Y_{0.06}Ga_{0.94})_2O_3$:Cr films we obtained. In particular, according to Ref. [25], when the number of growing grains leads to a 'matrix' of grains beyond statistical limits, a bimodal grain size distribution develops, which is called secondary grain growth. Grains that grow abnormally often have a limited or homogeneous texture.

Our results (Fig. 3) show that the distribution of grain diameters on the surface of the $(Y_{0.06}Ga_{0.94})_2O_3$:Cr film after argon heat treatment is described by a two-modal distribution with maxima in the region of 100 and 135 nm. This situation may indicate that grain growth occurred during the heat treatment due to growth and sintering processes. It should be noted that a similar situation is observed during RF deposition on similar υ-SiO_2 substrates and pure thin β-Ga_2O_3 films, where the growth of secondary and even tertiary grains is observed [26].

The luminescence spectra of the obtained thin $(Y_{0.06}Ga_{0.94})_2O_3$:Cr films under excitation by synchrotron radiation at 56 nm (22.14 eV) and 160 nm (7.75 eV) are shown in Fig. 4.

As can be seen from the results shown in Fig. 4, the spectra ob-

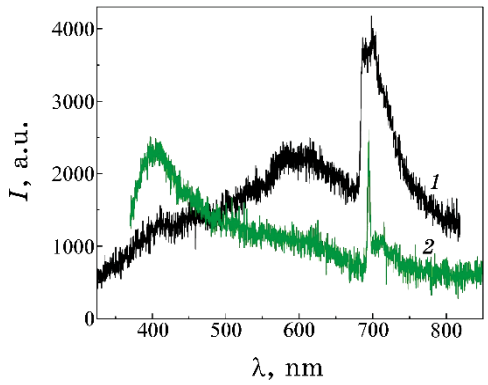

Fig. 4. The emission spectra of thin $(Y_{0.06}Ga_{0.94})_2O_3$:Cr films at $\lambda_{exc} = 56$ nm (*1*) and $\lambda_{exc} = 160$ nm (*2*) at 8.6 K.

tained at different excitation energies differ slightly. The luminescent luminescence spectrum under 56 nm excitation is characterised by intense luminescence in the 690–750 nm region with a maximum at 700 nm (1.77 eV) and a less intense band with a maximum at 600 nm (2.07 eV) and a local maximum in the luminescence spectrum at 400 nm (3.10 eV). When excited at 160 nm, a broad intense luminescence with a maximum in the 400 nm region, a local maximum in the 600 nm region, and a slight luminescence in the 690–750 nm region, which shows a narrow band with a maximum at 693.5 nm (1.788 eV), are observed.

The luminescent band with a maximum around 400 nm is a typical luminescence of the $(Y_{0.06}Ga_{0.94})_2O_3$ substrate, which was discussed in detail in Ref. [27]. This luminescence is also characteristic of pure β-Ga_2O_3 crystals [28, 29] and thin β-Ga_2O_3 films [30]. The luminescent band with a maximum in the region around 600 nm most likely corresponds to the luminescence of defects, primarily due to a disturbance in stoichiometry. This luminescence has not been reported in studies of nominally pure β-Ga_2O_3 crystals [28, 29] or the β-Ga_2O_3 and $(Y_{0.06}Ga_{0.94})_2O_3$ films [30], but it has been observed in thin $ZnGa_2O_4$:Cr films [31] and Y_2O_3:Cr^{3+} nanophosphors [32]. At the same time, as can be seen in Fig. 4, the luminescence intensity of luminescence and such defects depends on the energy of the excitation quanta. A similar situation is observed in the photoluminescence of $ZnGa_2O_4$:Cr [31].

The wide luminescence band in the 690–750 nm region is due to the intracentre luminescence of the Cr^{3+} impurity [33]. Gallium oxide has a monoclinic structure, and Cr^{3+} ions in the structure of β-Ga_2O_3 are in an octahedral oxygen environment [33]. In such an environment with an inversion centre, electrodipole transitions are

prohibited by parity. Therefore, the luminescent spectrum can be caused either by the displacement of chromium ions from the inversion centre or by interaction with crystal lattice vibrations. The indicated broad band of luminescence arises from the radiative transition $^4T_2 \rightarrow {}^4A_2$ [33] in Cr^{3+} ions. Against the background of this band, two narrow R-lines (R_1 and R_2), characteristic of Cr^{3+} ions in an octahedral environment, are distinguished in the short-wave region. The spectral position of these lines depends significantly on the temperature and the perfection of the samples obtained. In particular, with a decrease in temperature, the maxima of the R_1- and R_2-lines shift to the short-wave (high-energy) region [36–39]. In addition, our studies show that the cooling of β-Ga_2O_3:Cr^{3+} crystals to lower liquid nitrogen temperatures leads to a sharp decrease in the luminescence yield of the $^4T_2 \rightarrow {}^4A_2$ transition, quenching of the R_2 line, and a strong increase in the intensity of the R_1 line [36–39]. Our results are in good agreement with the above results and show that the intensity of the $^4T_2 \rightarrow {}^4A_2$ transition is determined not only by the temperature but also by the excitation energy.

A characteristic feature of the results of the study of the luminescence of β-Ga_2O_3:Cr^{3+} crystals at temperatures of 20 K and lower [36–39] is the presence of an intense luminescence of the R_1 line, the spectral position of which differs slightly from one author to another. In particular, in Ref. [36], the spectral position of the R_1 band is of 695.3 nm; in Ref. [37], it is of 695.6 nm; in Ref. [38], it is of 694.5 nm; and in Ref. [39], it is of 696.1 nm. Most likely, this situation is due to the structural perfection of the studied samples in different works. At the same time, in the obtained luminescence spectra of thin $(Y_{0.06}Ga_{0.94})_2O_3$:Cr^{3+} films, the spectral position of the R_1 band is even more energetic, *i.e.*, of 693.5 nm. Such a shift could be explained by the addition of Y^{3+} ions to the structure of β-Ga_2O_3 instead of some Ga^{3+} ions. However, this situation seems unlikely. Unfortunately, we have not found any scientific publications devoted to the low-temperature luminescence of Y_2O_3:Cr^{3+}. However, studies of such luminescence at room temperature [32] show that the spectral position of the R_1 line in the luminescence spectra of Y_2O_3:Cr^{3+} is more than 700 nm. At the same time, at room temperature, the position of the R_1-line varies from 695.6 nm [38] to 694.5 nm [39] depending on the perfection of the β-Ga_2O_3:Cr^{3+} samples. Therefore, the replacement of some Ga^{3+} ions with Y^{3+} ions should shift the R_1-band to a longer wavelength region, but the opposite situation is observed.

To analyse the observed high-energy shift in the spectral position of the R_1 band in the low-temperature luminescence spectra of thin $(Y_{0.06}Ga_{0.94})_2O_3$:Cr^{3+} films, we assume that they consist of nanocrystalline grains, for which a size effect is possible. The main reason

for such effects is the influence of surface energy. In a review article [40], the authors point out that the source of the change in surface energy is a large number of incomplete broken bonds. In this case, the smaller the size of the nanoparticle, the more such bonds account for the total number of bonds in the nanocrystal. That is, as the particle diameter decreases, the surface energy also decreases.

According to Ref. [41], a decrease in surface energy increases the volume of a unit cell. Therefore, in thin films consisting of nanocrystalline grains, the metal–ligand (Cr–O) distance increases and, as a result, the crystal field strength decreases, and the position of the emission bands is shifted. This situation, in particular, is observed in thin films of β-Ga_2O_3:Cr, where the crystal field strength is $D_q = 1667$ cm^{-1} [31]. The calculations of D_q in single-crystal samples of β-Ga_2O_3:Cr^{3+} [42] give the value of $D_q = 1680.7$ cm^{-1}.

An increase in the metal–ligand (Cr–O) distance leads to a change in the Raká parameters, which may result in a nephelauxetic effect. The term 'nephelauxetic' was introduced by Jørgensen in Ref. [43] to describe the expansion of the 3*d*-electron cloud, when a metal ion is in a crystal lattice. For a metal ion in a crystal lattice, the electrostatic repulsion between these electrons is weaker, and the electron-to-electron repulsion parameter Raká B decreases. A simple phenomenological description of this effect was proposed in Ref. [43]:

$$B = \beta B_0, \tag{1}$$

where B_0 is the Raká's parameter of the free ion and β is the proportionality coefficient, called the nephelauxetic parameter. In Ref. [44], certain limitations of the relation (1) were noted, and an extended form of the nephelauxetic parameter was proposed, which takes into account both the Raká's parameters B and C, in particular,

$$\beta_1 = \sqrt{\frac{B}{B_0} + \frac{C}{C_0}}, \tag{2}$$

where C_0 is the Raká's parameter of the free ion.

When the Cr^{3+} ion is in the $^4A_2$ ground state, three 3*d*-electrons occupy orbitals stretched in the directions between the ligands. As the ligands approach the metal ion (Cr–O), the bonds become more covalent, the 3*d*-electrons move further away, and the B parameter decreases. This leads to an increase in the distance between the $^4A_2$ ground state and the excited ^2E state. Given that, the excited ^2E

state splits in the crystal field into two sublevels, $\bar{E}$ and $2\bar{A}$, we observe two R-lines in the luminescence spectra.

Since, by definition, the nephelauxetic effect is manifested in a decrease in the Raká's B parameter and an increase in the C parameter with a decrease in the metal–ligand distance, *i.e.*, with an increase in the size of crystallites, we observe the presence of such an effect at a short-wave shift of the R_1 line in the luminescence spectra of thin films of $(Y_{0.06}Ga_{0.94})_2O_3$:Cr compared to single crystal samples. Given that, for example, the grain diameters vary from 25 to 170 nm (Fig. 3), this shift is considered as an average result due to the different magnitude of the nephelauxetic effect in crystallites of different sizes.

4. CONCLUSIONS

It has been established that thin films of $(Y_{0.06}Ga_{0.94})_2O_3$:Cr with an average surface roughness of 2.9 nm are formed on υ-SiO_2 substrates after heat treatment in argon, which are formed from nanocrystalline grains with an average diameter of 123 nm.

It is shown that, at low-temperature luminescence of thin $(Y_{0.06}Ga_{0.94})_2O_3$:Cr films, the shape of the luminescence spectrum depends on the energy of the excitation quanta, and the spectrum shows the luminescence of the $(Y_{0.06}Ga_{0.94})_2O_3$ in the form of a broad band with a maximum in the region of 400 nm, the luminescence of defects according to stoichiometry in a band with a maximum in the region of 600 nm and the activator luminescence of Cr^{3+} ions in the region of 690–750 nm, in which an intense R_1 line is distinguished. The maximum of this band was shifted to the high-energy region relative to single crystal samples. The analysis of this shift is based on the fact that at smaller sizes of nanocrystals in thin films relative to single crystals, the influence of surface energy is observed, since the number of elementary cells in nanocrystals decreases and the relative number of elementary cells on the surface of the crystallite increases proportionally. As a result, the volume of the unit cell increases, and the Cr–O distance increases accordingly. The consequence is the weakening of the ligand field and the appearance of a nephelauxetic effect, which leads to a high-energy shift of the R_1 band in the activator luminescence of thin $(Y_{0.06}Ga_{0.94})_2O_3$:Cr^{3+} films at a low temperature of 8.6 K.

ACKNOWLEDGEMENTS

The authors would like to thank Prof. T. M. Demkiv for the measurements of the luminescence spectra.

REFERENCES

1. Z. Galazka, S. Ganschow, A. Fiedler, R. Bertram, D. Klimm, K. Irmscher, R. Schewski, M. Pietsch, M. Albrecht, and M. Bickermann, *J. Cryst. Growth*, **486**: 82 (2018); https://doi.org/10.1016/j.jcrysgro.2018.01.022
2. M. He, Q. Zeng, and L. Ye, *Crystals*, **13**, No. 10: 1434 (2023); https://doi.org/10.3390/cryst13101434
3. V. Vasyltsiv, A. Luchechko, Y. Zhydachevskyy, L. Kostyk, R. Lys, D. Slobodzyan, R. Jakieła, B. Pavlyk and A. Suchocki, *J. Vacuum Science & Technol. A*, **39**, No. 3: 033201 (2021); https://doi.org/10.1116/6.0000859
4. S. Kumar and R. Singh, *phys. status solidi (RRL)*, **7**, No. 10: 781 (2013); https://doi.org/10.1002/pssr.201307253
5. E. Nogales, J. A. García, B. Méndez, and J. Piqueras, *J. Appl. Phys.*, **101**, No. 3: 033517 (2007); https://doi.org/10.1063/1.2434834
6. S. M. Xu, W. Ge, X. Zhang, P. Zhang, and Y. Li, *J. of Luminescence*, **246**, 118831 (2022); https://doi.org/10.1016/j.jlumin.2022.118831
7. R. Suzuki, S. Nakagomi, Y. Kokubun, N. Arai, and S. Ohira, *Appl. Phys. Lett.*, **94**, No. 22: 222102 (2009); https://doi.org/10.1063/1.3147197
8. O. M. Bordun, B. O. Bordun, I. Yo. Kukharskyy, and I. I. Medvid, *J. Appl. Spectrosc.*, **86**, No. 6: 1010 (2020); https://doi.org/10.1007/s10812-020-00932-4
9. D. Guo, Q. Guo, Z. Chen, Z. Wu, P. Li, and W. Tang, *Materials Today Physics*, **11**: 100157 (2019); https://doi.org/10.1016/j.mtphys.2019.100157
10. M. Alonso-Orts, E. Nogales, J. M. San Juan, M. L. Ny, J. Piqueras, and B. Mėndez, *Phys. Rev. Appl.*, **9**: 064004 (2018); http://dx.doi.org/10.1103/PhysRevApplied.9.064004
11. M. Crozzolin, C. Belloni, J. Xu, T. Nakanishi, J. Ueda, S. Tanabe, F. Dallo, E. Balliana, A. Saorin, F. Rizzolio, D. Cristofori, P. Riello, A. Benedetti, and M. Back, *J. Mater. Chem. C*, **12**, No. 29: 10929 (2024); doi:10.1039/D4TC01386G
12. D. M. Esteves, A. L. Rodrigues, L. C. Alves, E. Alves, M. I. Dias, Z. Jia, W. Mu, K. Lorenz, and M. Peres, *Scientific Reports*, **13**: 4882 (2023); https://doi.org/10.1038/s41598-023-31824-0
13. T. Minami, T. Nakatani, and T. Miyata, *J. Vac. Sci. Technol. A*, **18**, No. 4: 1234 (2000); https://doi.org/10.1116/1.582332
14. A. K. Saikumar, Sh. D. Nehate, and K. B. Sundaram, *ECS J. of Solid State Science and Technol.*, **8**, No. 7: Q3064 (2019); https://doi.org/10.1149/2.0141907jss
15. O. M. Bordun, B. O. Bordun, I. I. Medvid, and I. Yo. Kukharskyy, *Acta Physica Polonica A*, **133**, No. 4: 910 (2018); https://doi.org/10.12693/APhysPolA.133.910
16. K. H. Choi and H. C. Kang, *Materials Letters*, **123**: 160 (2014); https://doi.org/10.1016/j.matlet.2014.03.038
17. T. Igarashi, M. Ihara, T. Kusunoki, K. Ohno, T. Isobe, and M. Senna, *Appl. Phys. Lett.*, **76**, No. 12: 1549 (2000); https://doi.org/10.1063/1.126092
18. C. B. Willingham, J. M. Wahl, P. K. Hogan, L. C. Kupferberg, T. Y. Wong, and A. M. De, *Proc. SPIE*, **5078**: 179 (2003); https://doi.org/10.1117/12.500986
19. O. M. Bordun, I. M. Bordun, and S. S. Novosad, *J. Appl. Spectr.*, **62**, No. 6:

1060 (1995); https://doi.org/10.1007/BF02606760
20. E. F. Armendáriz-Alonso, O. Meza, E. G. Villabona-Leal, and Elías Pérez, *J. Sol–Gel Sci. and Technol.*, **111**: 216 (2024); https://doi.org/10.1007/s10971-024-06450-5
21. K. Wasa, M. Kitabatake, and H. Adachi, *Thin Film Materials Technology: — Sputtering of Compound Materials* (William Andrew Inc.: 2004)
22. O. M. Bordun, B. O. Bordun, I. J. Kukharskyy, I. I. Medvid, O. Ya. Mylyo, M. V. Partyka, and D. S. Leonov, *Nanosistemi, Nanomateriali, Nanotehnologii*, **17**, Iss. 1: 123 (2019); https://doi.org/10.15407/nnn.17.01.123
23. https://photonscience.desy.de/facilities/petra_iii/beamlines/p66_superlumi/index_eng.html
24. C. V. Thompson, *Solid State Phys.*, **55**: 269 (2001); https://doi.org/10.1016/S0081-1947(01)80006-0
25. C. V. Thompson, *J. Appl. Phys.*, **58**: 763 (1985); https://doi.org/10.1063/1.336194
26. O. M. Bordun, B. O. Bordun, I. Yo. Kukharskyy, I. I. Medvid, I. I. Polovynko, Zh. Ya. Tsapovska, and D. S. Leonov, *Nanosistemi, Nanomateriali, Nanotehnologii*, **19**, Iss. 1: 159 (2021); https://doi.org/10.15407/nnn.19.01.159
27. O. M. Bordun, I. I. Medvid, I. Yo. Kukharskyy, and B. O. Bordun, *Phys. and Chem. of Solid State*, **17**, No. 1: 53 (2016); https://doi.org/10.15330/pcss.17.1.53-59
28. E. Nogales, B. Méndez, and J. Piqueras, *Appl. Phys. Lett.*, **86**, No. 11: 113112 (2005); https://doi.org/10.1063/1.1883713
29. H. Tang, N. He, Z. Zhu, M. Gu, B. Liu, J. Xu, M. Xu, L. Chen, J. Liu, and X. Ouyang, *Appl. Phys. Lett.*, **115**, No. 11: 071904 (2019); https://doi.org/10.1063/1.5110535
30. O. M. Bordun, B. O. Bordun, I. Yo. Kukharskyy, and I. I. Medvid, *J. Appl. Spectrosc.*, **84**, No. 1: 46 (2017); https://doi.org/10.1007/s10812-017-0425-3
31. O. M. Bordun, V. G. Bihday, and I. Yo. Kukharskyy, *J. Appl. Spectrosc.*, **80**, No. 5: 721 (2013); https://doi.org/10.1007/s10812-013-9832-2
32. J. B. Prasanna Kumar, G. Ramgopal, D. V. Sunitha, B. Daruka Prasad, H. Nagabhushana, Y. S. Vidya, K. S. Anantharaju, S. C. Prashantha, S. C. Sharma, and K. R. Prabhakara, *Luminescence: J. Biol. Chem. Lum.*, **32**, No. 3: 414 (2017); https://doi.org/10.1002/bio.3197
33. O. M. Bordun, B. O. Bordun, I. Yo. Kukharskyy, D. M. Maksymchuk, and I. I. Medvid, *Phys. and Chem. of Solid State*, **24**, No. 3: 490 (2023); https://doi.org/10.15330/pcss.24.3.490-494
34. R. Rao, A. M. Rao, B. Xu, J. Dong, S. Sharma, and M. K. Sunkara, *J. Appl. Phys.*, **98**, No. 9: 094312 (2005); https://doi.org/10.1063/1.2128044
35. B. M. Weckhuysen, P. Van Der Voort, and G. Catana, *Spectroscopy of Transition Metal Ions on Surfaces* (Leuven University Press: 2000).
36. A. Luchechko, V. Vasyltsiv, Ya. Zhydachevskyy, M. Kushlyk, S. Ubizskii, and A. Suchocki, *J. Phys. D: Appl. Phys.*, **53**, No. 35: 354001 (2020); https://doi.org/10.1088/1361-6463/ab8c7d
37. Y. Tokida and S. Adachi, *J. Appl. Phys.*, **112**, No. 6: 063522 (2012); https://doi.org/10.1063/1.4754517
38. C. Remple, L. M. Barmore, J. Jesenovec, J. S. McCloy, and M. D. McCluskey, *J. Vac. Sci. Teshnol. A*, **41**: 022702 (2023);

https://doi.org/10.1116/6.0002340
39. H. Yusa and M. Miyakawa, *J. Appl. Phys.*, **137**, No. 3: 035902 (2025); https://doi.org/10.1063/5.0246260
40. D. Vollath, F. D. Fischer, and D. Holec, *Beilstein J. Nanotechnol.*, **9**: 2265 (2018); https://doi.org/10.3762/bjnano.9.211
41. P. J. Dereń, A. Watras, and D. Stefańska, *Opt. Spectrosc.*, **131**: 795 (2023); https://doi.org/10.1134/S0030400X23070032
42. J. G. Zhang, B. Li, C. T. Xia, J. Xu, Q. Deng, X. D. Xu, F. Wu, W. S. Xu, H. S. Shi, G. Q. Pei, and Y. Q. Wu, *Sci. China Ser. E-Tech. Sci.*, **50**, No. 1: 51 (2007); https://doi.org/10.1007/s11431-007-2026-5
43. C. K. Jørgensen, *The Nephelauxetic Series P. 73–124 Progress in Inorganic Chemistry* (Ed. F. A. Cotton) (New York–London: Interscience Publishers: 1962), vol. **4**.
44. M. G. Brik, S. J. Camardello, A. M. Srivatsava, N. M. Avram, and A. Suchotcki, *ECS J. Solid State. Sci. Technol.*, **5**: R3067 (2016); https://doi.org/10.1149/2.0091601jss